7614–7625 *Nucleic Acids Research, 2007, Vol. 35, No. 22* *Published online 2 November 2007*
doi:10.1093/nar/gkm917

Ribonuclease P processes polycistronic tRNA transcripts in *Escherichia coli* independent of ribonuclease E

Bijoy K. Mohanty and Sidney R. Kushner*

Department of Genetics, University of Georgia, Athens, GA 30602, USA

Received August 6, 2007; Revised October 3, 2007; Accepted October 9, 2007

ABSTRACT

The first step in the current model for the processing and maturation of mono- and polycistronic tRNA precursors in *Escherichia coli* involves initial cleavages by RNase E 1–3 nt downstream of each chromosomally encoded CCA determinant. Subsequently, each mature 5′ terminus is generated by single RNase P cleavage, while the 3′ terminus undergoes exonucleolytic processing by a combination of 3′ → 5′ exonucleases. Here we describe for the first time a previously unidentified pathway for the maturation of tRNAs in polycistronic operons (*valV valW* and *leuQ leuP leuV*) where the processing of the primary transcripts is independent of RNase E. Rather, RNase P cleavages separate the individual tRNA precursors with the concomitant formation of their mature 5′ termini. Furthermore, both polynucleotide phosphorylase (PNPase) and RNase II are required for the removal of the 3′ Rho-dependent terminator sequences. Our data indicate that RNase P substrate recognition is more complex than previously envisioned.

INTRODUCTION

Transfer RNAs (tRNAs) serve as adapter molecules for translating the genetic code into protein sequences. In *Escherichia coli*, the 86 tRNA genes are frequently embedded in complex operons containing either other tRNAs, rRNAs (ribosomal RNAs) or mRNAs (messenger RNAs) (1). All the tRNA genes, including those that are monocistronic, are transcribed as precursors that undergo a series of processing steps at both their 5′ and 3′ termini to produce the mature species that are substrates for the respective tRNA synthetases.

Extensive studies on the enzymes associated with the maturation of the 5′ and 3′ termini of tRNAs in *E. coli* (2–5) have led to a consensus pathway by which it is believed that every tRNA precursor is matured (6). Specifically, this model states that for both mono- and polycistronic precursors RNase E is required to generate pre-tRNAs that contain a limited number of extra nucleotides at their 5′ and 3′ termini (6–9) (Figure 1). However, the observation of considerable differences in the efficiency of RNase E cleavage among a large number of tRNA precursors (8) suggested that tRNA abundance was primarily controlled either by the differences in the cleavage specificity of RNase E for the primary transcripts and/or the existence of a processing pathway that was independent of RNase E. In fact, a recent study by Deana and Belasco (10) suggested the existence of an alternative processing mechanism for RNase E-dependent tRNAs in *rne-1* mutants that did not involve its homolog, RNase G. However, they did not realize at that time that there is a significant amount of residual RNase E activity present in an *rne-1* strain at the non-permissive temperature (11).

The most promising candidate that could serve as an alternative processing enzyme is actually RNase P, a ribonucleoprotein that consists of a protein (C5) encoded by *rnpA* and an RNA (M1) subunit encoded by *rnpB* (12). The RNA component of the holoenzyme is responsible for the catalytic activity of the enzyme (13) and is found in all organisms (14). In fact, experiments conducted using a temperature-sensitive RNase P allele [*rnpA49*, a mutation of arginine to histidine in the C5 protein subunit (15)] have suggested that the enzyme is required to mature the 5′ terminus of all tRNA precursors and plays a role in cleaving some polycistronic mRNAs and tRNA precursors (16–22).

It has been suggested that the absence of RNase E inhibits RNase P activity (6–8), since RNase P has reduced activity when there are long 3′ precursor sequences (23). Thus it has been argued that in general RNase P generates the mature 5′ terminus only after an initial RNase E cleavage event (6,8,21). Subsequently, the mature 3′ terminus is obtained through the combined action of RNase T, RNase BN, RNase D, RNase II and RNase PH (3,6,24,25).

In this communication, we demonstrate a previously uncharacterized pathway for the processing of the *valV*

*To whom correspondence should be addressed. Tel: +1 706 542 8000; Fax: +1 706 542 3910; Email: skushner@uga.edu

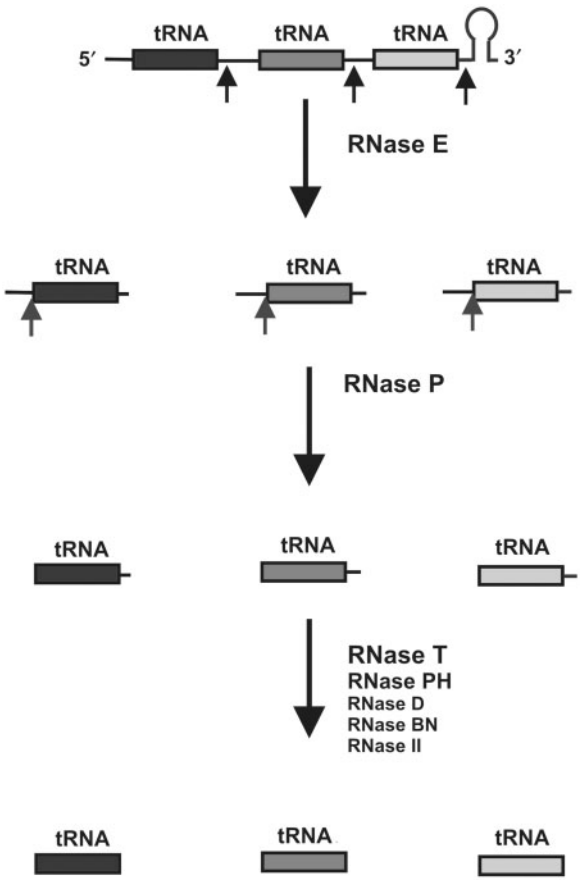

Figure 1. RNase E-dependent maturation of tRNA precursors. In operons such as *glyW cysT leuZ* and *argX hisR leuT proM*, RNase E initiates processing by cleaving 1–2 nt downstream of the CCA determinant of each tRNA within the operon (6) leading to the formation of immature tRNAs, which are further processed by RNase P to generate mature 5′ termini. The mature 3′ ends result primarily from the activity of RNase T, but RNase PH, RNase D, RNase BN and RNase II can substitute in the absence of RNase T (4).

valW and *leuQ leuP leuV* transcripts into their component pre-tRNAs that only involves RNase P. Using various experimental approaches, we show that the primary transcripts of these operons are dramatically stabilized in an *rnpA49* mutant with a concomitant decrease in the level of corresponding mature tRNAs. In contrast, no significant effect of RNase E was observed at any stage in the processing of these tRNAs. Furthermore, the predicted Rho-dependent terminators of both primary transcripts appeared to be primarily removed exonucleolytically by a combination of RNase II and PNPase.

MATERIALS AND METHODS

Bacterial strains and plasmids

The *E. coli* strains used in this study were all derived from MG1693 (*thyA715 rph-1*) provided by the *E. coli* Genetic Stock Center, Yale University. The *rne-1* and *rnpA49* alleles encode temperature-sensitive RNase E and RNase P proteins, respectively, that are unable to support cell viability at 44°C (22,26,27). SK5665 (*rne-1 thyA715 rph-1*) (26), SK2525 (*rnpA49 thyA715 rph-1 rbsD296*::Tn*10*) (8), SK2534 (*rne-1 rnpA49 thyA715 rph-1 rbsD296*::Tn*10*) (8), SK10019 (*pnp△683*) (28), CMA201 (*Δrnb thyA715 rph-1*) (29,30) and SK5726 (*pnp-7 rnb-500 thyA715 rph-1*) (31) have been previously described. A P1 lysate grown on SK2525 (*rnpA49 rbsD296::*Tn*10* was used to transduce both SK10019 (*pnpΔ683*) and SK5726 (*pnp-7 rnb-500*) to construct SK10443 (*rnpA49 thyA715 rph-1 rbsD296*::Tn*10 pnpΔ683*) and SK10451(*rnpA49 thyA715 rph-1 rbsD296*::Tn*10 pnp-7 rnb-500*), respectively.

Growth of bacterial strains and isolation of total RNA

Bacterial strains were routinely grown with vigorous shaking in Luria broth supplemented with thymine (50 μg/ml) at 30°C until they reached a cell density of 1×10^8/ml (40 Klett units above background, No. 42 green filter) after which the cultures were shifted to 44°C. For complete inactivation of the temperature-sensitive RNase E protein encoded by the *rne-1* allele (8), the cultures were maintained in exponential growth at 44°C for 2 h by periodic dilutions with fresh pre-warmed medium. When appropriate, tetracycline or streptomycin (20 μg/ml) were added to the medium. For half-life determinations, rifampicin (500 μg/ml, solubilized in dimethyl sulfoxide) and nalidixic acid (20 μg/ml) were added to the growing cultures at 50 Klett units and the first sample (0 min) was removed 75 s later. Total RNA was extracted as described previously (32). All RNA preparations were further treated with DNase I using the DNA-free kit™ (Ambion) to remove any residual DNA contamination. To ensure equal loading of all RNA samples during northern and primer extension analysis, each RNA sample was first quantified by measuring the OD_{260}. Subsequently, the RNA samples (500 ng) were normalized by quantifying Vistra Green (Amersham Bioscience) stained 16S and 23S rRNAs in agarose mini-gels using a PhosphorImager (Amersham Bioscience, Storm 840).

Northern analysis

Total RNA was separated in 6% polyacrylamide gels containing 8 M urea in TBE [Tris–Borate–EDTA buffer (33)]. The RNA was transferred onto Magnacharge nylon membranes (GE Water & Processing Technologies) by electroblotting in TAE (Tris–Acetate–EDTA) buffer and probed with appropriate ^{32}P-labeled oligonucleotides. Oligonucleotide probes were 5′ end-labeled with T4 polynucleotide kinase (NEB). In many cases, the same northern blot was probed successively with different oligonucleotides after stripping off the previous probe in boiling SDS (0.5%) solution. The prehybridization (4–5 h) and the hybridization of oligonucleotide probes (overnight) to the membrane were carried out using a hybridizing solution (2 × SSC, 0.2% SDS and 0.25% non-fat dry milk, autoclaved) at a temperature that was below 10°C of the T_m of the corresponding oligonucleotide. Each membrane was washed three times (15 min each in 0.3% SDS and 2 × SSC) at room temperature. Band intensities were quantitated with a PhosphorImager. The half-lives of the *valV valW* and *leuQ leuP leuV* tRNA

precursor transcripts in wild type and *rne-1* strains (Figures 4A and 6A) were conservatively estimated to be <30 s, since we could not see any transcripts at 0 min, which represented a period of only 75 s after following the addition of rifampicin.

Primer extension

Primer extension analysis of the *valV valW* operon was carried out essentially as described previously (34) with the following modifications. Sterile distilled water (80 µl) was added to each reverse transcription reaction mixture (20 µl) and the total volume extracted with 100 µl of phenol:chloroform (5 : 1, Ambion) solution. The reverse transcription products were precipitated at −20°C after the addition of 0.1 volume of sodium acetate (3 M, pH 5.2), 1 µl of GlycoBlue™ (Ambion) and 2.5 volume of ethanol (100%) to the aqueous supernatant. Each pellet was dissolved in 2.5 µl of the stop solution from the Promega *fmol*® DNA cycle sequencing kit. The nucleotide sequence was obtained from a PCR DNA product (amplified from wild-type genomic DNA using primers upstream and downstream of the *valV valW* operon) using the Promega *fmol* sequencing kit and the primer VALV-W (primer b, Figure 2A) that was also used for the reverse transcription. The sequences were analyzed on a 6% PAGE containing 8 M urea.

Oligonucleotide probes and primers

The sequences of all the oligonucleotides used in the experiments reported here are available on request.

RESULTS

Endonucleolytic processing of the *valV valW* transcript does not require RNase E

Although it has been shown by bioinformatics and biochemical analysis that RNase E is involved in the maturation of a large number of *E. coli* tRNAs (6,8,21), the fact that the enzyme appeared to process some tRNAs more efficiently than others (8) suggested the possibility of an alternative maturation pathway that did not involve RNase E. Furthermore, we noted that the intergenic region of the *valV* operon (containing *valV* and *valW*, which encodes $tRNA^{Val/GAC}$, Figure 2A) was only 4 nt in length (UCCU, Table 1) and did not contain an obvious A/U-rich RNase E cleavage site. In addition, unlike the transcripts of other operons that have been shown to be dependent on RNase E for their maturation (6,8), the *valV valW* transcript appeared to be terminated in a Rho-dependent fashion, since the downstream sequences do not contain any predicted secondary structures and the downstream gene (*ydhR*) is not cotranscribed with *valV valW* (data not shown). Accordingly, we analyzed the maturation of *valV valW* transcript using northern blot analysis with steady-state RNA isolated from a series of strains (wild-type, *rne-1*, *rnpA49* and *rne-1 rnpA49*) that had been shifted to 44°C for 120 min to inactivate the temperature-sensitive RNase E and RNase P proteins.

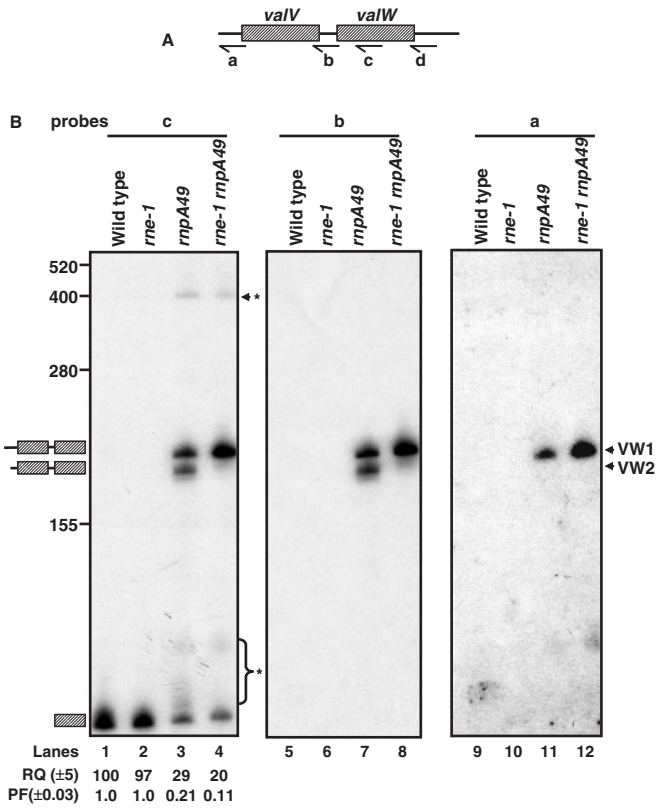

Figure 2. Analysis of the processing of *valV valW* operon. (**A**) Schematic representation of *valV valW* operon (not drawn to scale). Relative positions of the oligonucleotide probes (a: VALV-UP, b: VALV-W, c: VALW and d: VALW-TER) used in the northern analysis are shown below the diagram. (**B**) Northern analysis of *valV valW* operon. Total RNA (12 µg/lane) was separated on 6% PAGE, transferred to nylon membrane and probed multiple times as described in the Materials and Methods section. The autoradiograms shown were from the same blot successively probed with c, b and a. The genotypes of the strains used were noted against each lane. The RNA molecular weight (nts) size standards (Invitrogen) and the graphical structures of the *valV valW* processing intermediates are shown to the left. The names for the processing intermediates of *valV valW* transcripts are shown to the right. Relative quantity (RQ) of mature $tRNA^{Val}$ in various genetic backgrounds was calculated by setting the wild-type level at 1. Processed fraction (PF) denotes the fraction of a given mature tRNA relative to the total amount of that tRNA (processed and unprocessed) in the specific genetic background. RQ and PF were obtained from the average of two independent experiments. The bands marked with asterisks (*) on the c probed blot were due to weak hybridization to *val* operons independent of *valV valW*.

Since the coding sequences of *valV* and *valW* are nearly identical, but are considerably different from the remaining five $tRNA^{Val}$ genes (*valU*, *valX*, *valY*, *valT* and *valZ*), we initially probed the blot with an oligonucleotide complementary to both *valV* and *valW* (probe c, Figure 2A). As shown in Figure 2B, only the mature $tRNA^{Val}$ species was visible in the wild-type control and *rne-1* mutant (lanes 1–2). In striking contrast, the most prominent species in the *rnpA49* strain were two high molecular weight intermediates (VW1 and VW2) that appeared to contain both *valV* and *valW* based on their size (Figure 2B, lane 3). Interestingly, the level of VW1 increased ~3-fold and the VW2 transcript completely

Table 1. Comparison of nucleotide sequences downstream of CCA determinants in various tRNA genes

tRNA	Sequence	Known RNase E cleavage site	Reference
tyrT	CCA↓AAUUC	Yes	(6,8)
lysY	CCA↓UUUUA	Yes	(6,8)
hisR	CCA↓UUAUA	Yes	(6)
cysT	CCA↓UUCU	Yes	(6)
leuQ	CCAAACGAG	No	This study
leuP	CCAAAAACC	No	This study
leuV[a]	CCAAUUAUC	No	This study
valV	CCAUCCU**GC**[b]	No	This study
ValW[a]	CCAGAUUUU	No	This study

[a]This species is at the end of an operon. Sequences are part of the mature downstream tRNA. After *leuV* and *valW* there are unstructured Rho-dependent terminators (36).
[b]Bold letters represent the 5′ mature terminus of *valW*.

disappeared in the *rne-1 rnpA49* double mutant (Figure 2B, lane 4). Importantly, both the relative quantity (RQ) as well as the processed fraction (PF) of the two $tRNA^{Val}$ species encoded by *valV* and *valW* did not change significantly in the *rne-1* mutant compared to the wild-type control (Figure 2B, lanes 1–2). In contrast, both the RQ and PF of $tRNA^{Val}$ decreased between 5- and 10-fold in *rnpA49* mutant relative to the wild-type strain (Figure 2B, lanes 3–4).

We hypothesized that the additional low intensity bands present in the *rnpA49* and *rne-1 rnpA49* strains (Figure 2B, lanes 3–4, *) arose from weak hybridization of probe c to a $tRNA^{Val}$ coding sequence derived from a different operon. In order to confirm this and to determine the composition of the VW1 and VW2 transcripts more precisely, the blot was probed with the oligonucleotide b (Figure 2A), which was complementary to the intergenic region between *valV* and *valW* but would not hybridize to either the *valV* or *valW* mature tRNAS. In agreement with the results obtained with probe c, no transcripts were detected in either the wild-type or *rne-1* strains (Figure 2B, lanes 5–6). However, the two processing intermediates (VW1 and VW2) seen in Figure 2B (lanes 3–4) also accumulated in the *rnpA49* mutants (Figure 2B, lanes 7–8). Furthermore, the transcript VW2 was missing and the level of the VW1 intermediate increased ~3-fold in the *rne-1 rnpA49* double mutant compared to the *rnpA49* single mutant, similar to what was observed with probe c. Significantly, the other species (*) observed with probe c, were not detected (Figure 2B, lanes 7 and 8).

To assess the composition of the 5′ and 3′ termini of VW1 and VW2, additional probing was carried out with oligonucleotides a and d (Figure 2A). While probe a hybridized to VW1 only, (Figure 2B, lanes 9–12), probe d failed to detect either of the processing intermediates (data not shown). This indicated that VW1 retained the complete 5′ leader sequence but was missing the 3′ downstream sequences associated with the Rho-dependent transcription terminator. In contrast, VW2 missed both the 3′ downstream sequences as well some portion of the 5′ leader region.

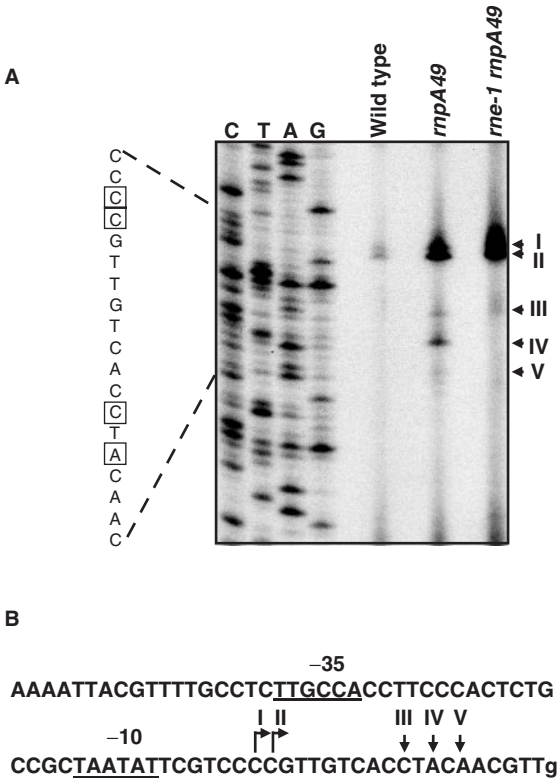

Figure 3. Primer extension analysis to determine the 5′ ends of *valV valW* transcripts. (**A**) Autoradiograph of the primer extension analysis. The reverse transcription products of total RNA (10 μg/lane) isolated from wild-type (MG1693), *rnpA49* (SK2525) and *rne-1 rnpA49* (SK2534) strains using the primer b (Figure 1A) were separated on a 6% PAGE as described in the Materials and Methods section. The CTAG sequencing reactions were carried out using the same primer and a PCR DNA fragment containing *valV valW* operon as template. The two transcription initiation sites (I and II) and three RNase E endonucleolytic cleavage sites (III, IV and V) are indicated. Part of the nucleotide sequences showing the primer termination sites (boxed nucleotides) sites are also shown. (**B**) The nucleotide sequences of the promoter regions of *valV valW* operon showing the determined transcription start (bent arrows) and endonucleolytic processing (arrows) sites. Lower case g is the 5′ mature end of *valV* tRNA. The putative −10 and −35 sequences (underlined) are shown.

RNase E cleaves inefficiently in the non-A/U-rich 5′ leader of the *valV valW* transcript in an *rnpA49* mutant

The data described in Figure 2B indicated that the VW2 intermediate seen in the *rnpA49* single mutant (Figure 2B, lanes 3 and 7) arose from RNase E cleavage(s) in the 5′ leader region of VW1, since this species was missing in the *rnpA49 rne-1* double mutant (Figure 2B, lanes 4 and 8). Accordingly, the 5′ termini of the *valV valW* transcripts were determined in wild-type, *rnpA49* and *rne-1 rnpA49* strains using primer extension analysis. Two primer extension products (I and II) terminating at positions 18 (C) and 19 (C) nt, respectively, upstream of the 5′ mature end of $tRNA^{Val}$ were detected in the wild-type strain (Figure 3A). Since no other larger products were observed, I and II represented two distinct transcription initiation sites for the *valV valW* transcript. This conclusion was supported by the presence of upstream consensus

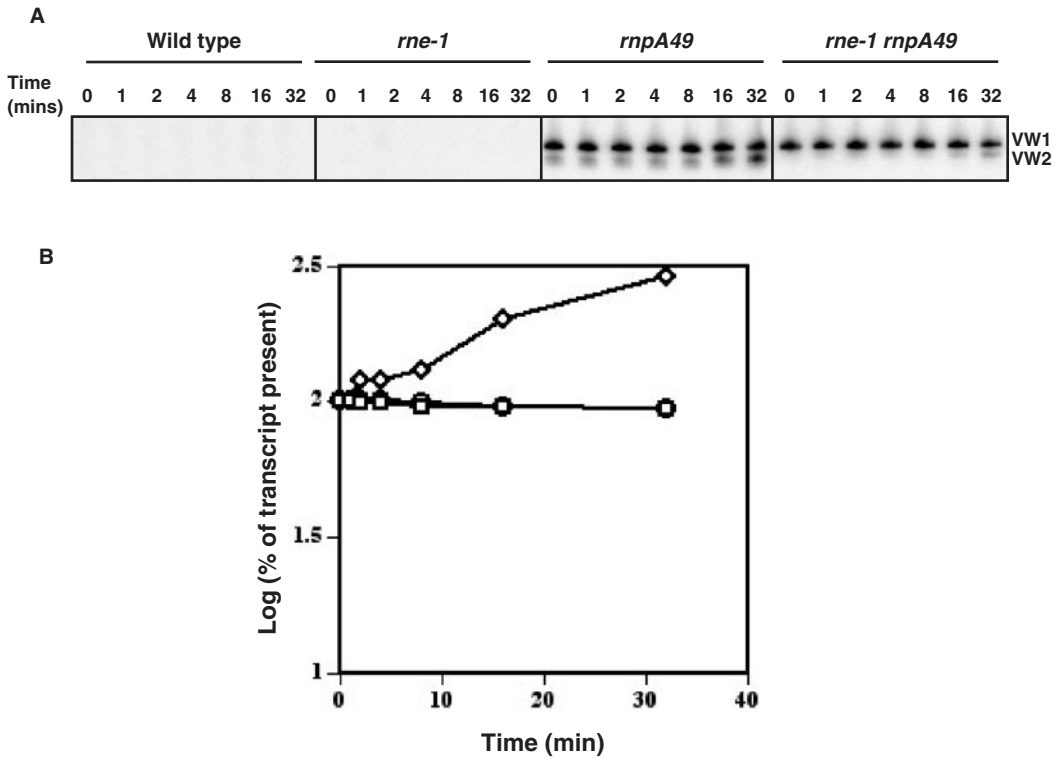

Figure 4. Decay of the processing intermediates of *valV valW* operon. (**A**) Autoradiogram of northern analysis showing the decay of *valV valW* transcripts (VW1 and VW2) in the wild type (MG1693), *rne-1* (SK5665), *rnpA49* (SK2525) and rne-*1 rnpA49* (SK2534) mutants. Total RNA (1 μg/lane) from different strains was isolated at times (minutes after rifampicin addition) indicated at the top of the blot and was separated on 6% PAGE, transferred to nylon membrane and probed with probe b (Figure 2A) as described in the Materials and Methods section. Two northern blots (one for wild type and *rne-1* and another for *rnpA49* and *rne-1 rnpA49* strains) were run independently. (**B**) A graphical presentation of the amounts of VW1 (open square: *rnpA49*, open circle: *rne-1 rnpA49*) and VW2 (open diamond: *rnpA49*) in various genetic backgrounds. The intensity of the bands in (A) was quantified with a Storm 840 PhosphorImager (Amersham Bioscience) and the values (log of the percentage of transcript present compared to the 0 min time point) were plotted as a function of time.

−10 (4/6) and −35 (5/6) sequences associated with a σ^{70} promoter (Figure 3B).

Consistent with the northern analysis (Figure 2B), the level of primer extension products (I and II) increased dramatically in both the *rnpA49* single and *rne-1 rnpA49* double mutants compared to the wild-type control (Figure 3A). In addition, three additional major primer extension products (III-V) located 10, 8 and 6 nt upstream of the 5′ mature end of $tRNA^{Val}$ were reproducibly detected in the *rnpA49* mutant (Figure 3B). Bands IV and V were absent and the intensity of band III was reduced in both the wild-type and *rne-1 rnpA49* strains (Figure 3A), suggesting that they were generated only in the absence of RNase P by inefficient RNase E cleavages within a non-A/U-rich region (Figure 3B).

Inactivation of RNase P dramatically stabilizes the *valV valW* transcript

It has been noted previously that the half-lives of most *E. coli* tRNA precursors are so short that it is not possible to accurately measure them in wild-type cells (8). In agreement with these results, we could not determine a half-life for the processing intermediates VW1 and VW2 in either wild type or *rne-1* strains (Figure 4A). However, in both the *rnpA49* and *rne-1 rnpA49* strains, the VW1 transcript had a half-life of >32 min (Figure 4A and B). Interestingly, there was a slow accumulation of the VW2 species in the *rnpA49* strain that was significantly reduced in the *rnpA49 rne-1* double mutant (Figure 4A and B).

RNase P is essential for the endonucleolytic processing of the *leuQ leuP leuV* primary transcript

In determining if transcripts from additional polycistronic tRNA operons might be endonucleolytically matured exclusively by RNase P, we noted from previous studies that several high molecular weight species containing leucine tRNAs accumulated at the non-permissive temperature in an *rnpA49* mutant (19,20). Of the six leucine tRNAs, the operons containing *leuT* and *leuZ* have been shown to be dependent on RNase E for initial processing (6,8). However, when we visually inspected the sequence of the *leuQ leuP leuV* operon that encodes three $tRNA^{Leu1}$ in tandem (Figure 5A), we noticed that there were no U residues immediately downstream of either the mature *leuQ* (CCAAAAACC) or *leuP* (CCAAACGAG) encoded tRNAs (Table 1). This observation was of particular interest, since all the currently mapped RNase E cleavage sites in tRNA precursors occur within A/U-rich sequences immediately downstream of the CCA determinants (Table 1).

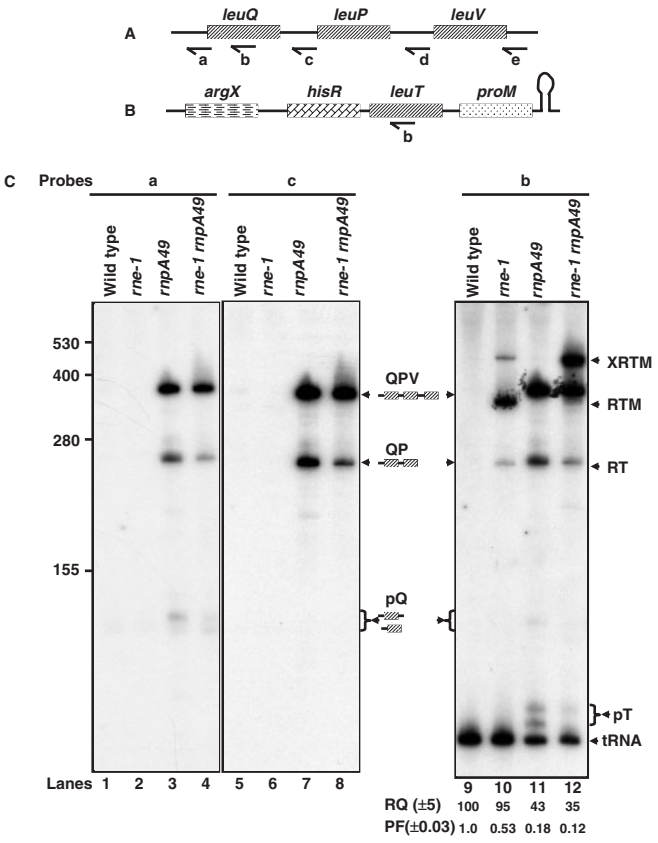

Figure 5. Analysis of the processing of $tRNA^{Leu1}$. (**A**) Schematic presentation of the *leuQ leuP leuV* (A) and *argX hisR leuT proM* (B) operons (not drawn to scale). The leucine tRNA genes are shaded the same to reflect their identical nucleotide sequences. Relative positions of the oligonucleotide probes (a: LEUQ-UP, b: LEUQ, c: LEUQ-P, d: LEUP-V and e: LEUV-TER) used in the northern analysis are shown below the diagram. (**B**) Northern analysis of *leuQ leuP leuV* operon. Total RNA (1 μg/lane) was separated on 6% PAGE, transferred to nylon membrane and probed as described in the Materials and Methods section. The autoradiograms shown were from the same blot probed sequentially with a, c and b. The genotypes of the strains used are noted against each lane. The RNA molecular weight (nts) size standards (Invitrogen) are shown to the left. The structures and the names for the processing intermediates of *leuQPV* transcript are shown. The bands labeled as XRTM, RTM, RT and pT on the b probed blot were identified using *argX* operon (*argX hisR leuT proM*) specific probes (data not shown) which represented additional processing intermediates of *argX* operon and were identical to the previous report (6). Species RT and QP have very similar molecular weights. XRTM: *argX hisR leuT proM*, RTM: *hisR leuT proM*, RT: *hisR leuT* and pT: pre-*leuT*. RQ and PF are described in Figure 1.

Since there are four loci for $tRNA^{Leu1}$ and one of them (*leuT*) is part of a different polycistronic tRNA operon (*argX hisR leuT proM*, Figure 5B), we initially analyzed a northern blot using intergenic probes (Figure 5A) to specifically identify the composition of the processing intermediates derived from the *leuQ leuP leuV* transcript. No transcripts were detected in either the wild-type or *rne-1* strains using probes a, c, d and e (Figure 5A and C, lanes 1–2, 5–6 and data not shown).

However, probes a, c and d hybridized to one or more high molecular weight intermediates in the *rnpA49* mutant (Figure 5C, lanes 3 and 7, data not shown), while probe e failed to detect any transcripts in all four genetic backgrounds tested (data not shown). Thus the largest species, labeled QPV in Figure 5C contained the intact 5′ leader region as well as the coding sequences of *leuQ*, *leuP* and *leuV* but not the 3′ downstream sequences. Likewise, the transcript labeled QP was missing the last tRNA (*leuV*) based on its hybridization to probes a–c but not d (Figure 5C, lanes 3 and 7 and data not shown). Similarly, the transcripts labeled pQ (Figure 5C, lane 3) missed the last two tRNAs (*leuP* and leuV), since they did not hybridize to probe c (Figure 5C, lane 7). Finally, the hybridization of probe a to all four bands (QPV, QP and pQ) suggested that all the intermediates retained the 5′ unprocessed sequence of the *leuQ leuP leuV* operon.

To determine the origin of QP and pQ bands, we also examined steady-state RNA isolated from an *rnpA49 rne-1* double mutant. While the amounts of the QPV transcript were comparable in the *rnpA49* and *rnpA49 rne-1* strains, the levels of the QP and pQ intermediates were reduced 2-fold in the double mutant compared to the *rnpA49* single mutant (Figure 5C, lanes 4 and 8). Quantitatively, the amount of the QP and pQ bands represented $27 \pm 3\%$ of the total hybridization in the *rnpA49* strain compared to only $18 \pm 2\%$ in the *rnpA49 rne-1* double mutant (Figure 5C, lanes 3, 4, 7 and 8), indicating the occurrence of inefficient RNase E cleavages in the intergenic regions of the QPV transcript in the absence of RNase P.

As mentioned above, there are four genes (*leuQ*, *leuP*, *leuV* and *leuT*) that encode $tRNA^{Leu1}$. Since *leuT* is part of the *argX hisR leuT proM* operon that is dependent on RNase E for its processing (6,8), probe b (Figure 5A and B) offered the opportunity to both establish the importance of RNase P in the production of mature $tRNA^{Leu1}$ as well as providing an internal control to distinguish between RNase E- and RNase P-dependent processing.

As expected, probe b hybridized to mature $tRNA^{Leu1}$ in all four strains (Figure 5C, lanes 9–12). In fact, several processing intermediates associated with the *argX* operon accumulated in the *rne-1* strain but were completely absent in the *rnpA49* mutant (Figure 5C, lane 10, XRTM, RTM and RT) (6,8). On the other hand, the processing intermediates QPV, and pQ, which are part of the *leuQ leuP leuV* operon only accumulated in the *rnpA49* mutant (Figure 5C, lane 11) as was also observed in lanes 3 and 7 (Figure 5C). It should be noted that band RT (containing *hisR leuT*) from the *argX* operon and band QP (containing *leuQ leuP*) from the *leuQ leuP leuV* operon have identical molecular weights resulting in their overlap in the *rnpA49* mutant (Figure 5C, lanes 10–11). Band RT was specifically identified by probing with a *hisR*-specific oligo (data not shown). The new smaller species in the *rnpA49* single mutant (pT, Figure 5B, lane 11) were $tRNA^{Leu1}$ precursors that were 10–15 nt longer than the mature species, which were likely generated by RNase E cleavages upstream and downstream of *leuT* (6,11). This interpretation was supported by the fact that the intermediates XRTM, RTM and TM disappeared in the *rnpA49 rne-1* double mutant along with a concomitant increase in the full-length *argX* operon transcript (XRTM, Figure 5B, lane 12).

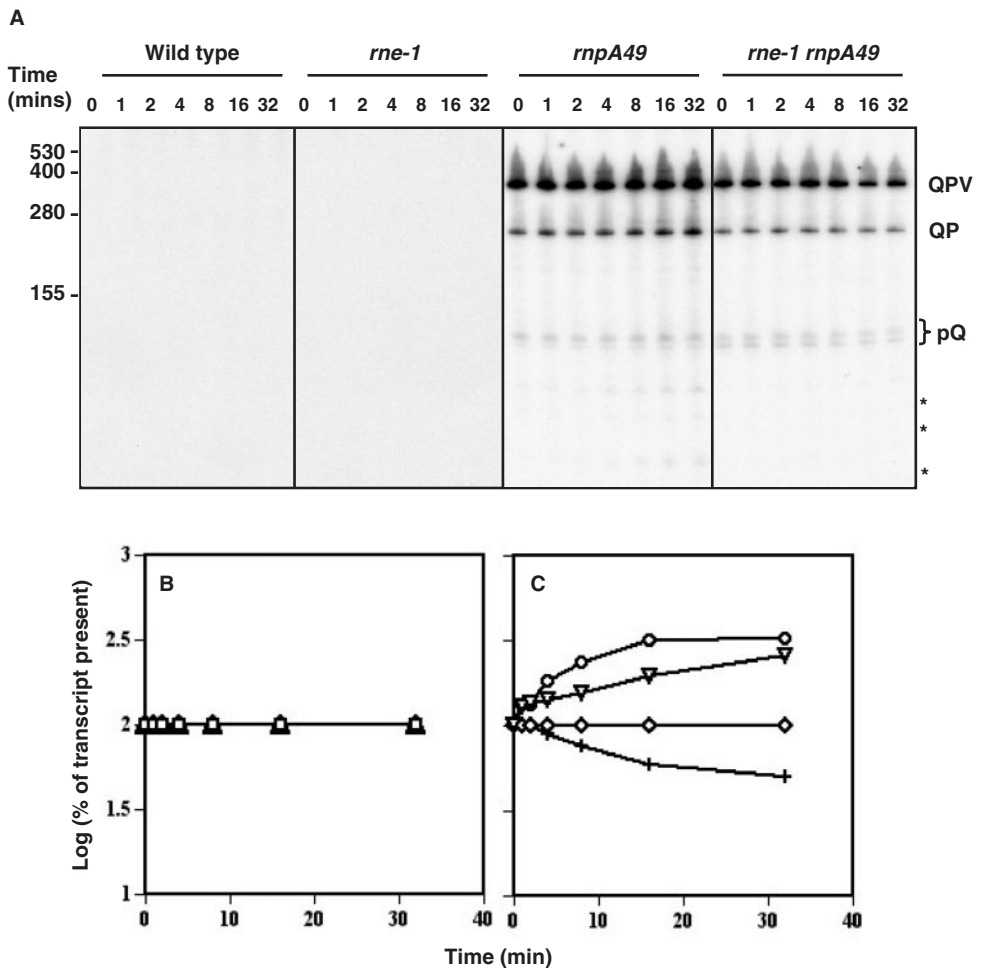

Figure 6. Decay of the processing intermediates of *leuQ leuP leuV* operon. (**A**) Autoradiogram of northern analysis showing the decay of *leuQ leuP leuV* transcripts (QPV, QP and pQ) in the wild type (MG1693), *rne-1* (SK5665), *rnpA49* (SK2525) and *rne-1 rnpA49* (SK2534) mutants. Total RNA (1 μg/lane) from different strains was isolated at times (minutes after rifampicin addition) indicated at the top of the blot and was separated on 6% PAGE, transferred to nylon membrane and probed with probe a (Figure 5A). The RNA molecular weight (nts) size standards (Invitrogen) are shown to the left. Asterisk (*) indicates the break-down products in *rnpA49* mutant not present in *rne-1 rnpA49* double mutant. Two northern blots (one for wild type and *rne-1* and another for *rnpA49* and *rne-1 rnpA49* strains) were run independently. (**B** and **C**) A graphical presentation of the amounts of QPV (open square: *rnpA49*,open triangle: *rne-1 rnpA49*), QP (inverted triangle: *rnpA49*, open diamond: *rne-1 rnpA49*) and pQ (open circle: *rnpA49*, +: *rne1 rnpA49*) in various genetic backgrounds. The band intensities in (A) were quantified with a PhosphorImager and the values (log of the percentage of transcript present compared to the 0 min time point) were plotted as a function of time.

Not surprisingly, the PF (processed fraction) of $tRNA^{Leu1}$ only decreased to 0.53 in the *rne-1* strain, but dropped more than 5-fold in the *rnpA49* mutants (Figure 5C, lanes 11–12) compared to the wild-type strain (Figure 5C, lane 9). Similarly, the relative quantity (RQ) of the mature $tRNA^{Leu1}$ only decreased marginally in the *rne-1* mutant (Figure 5C, lane 10), but dropped dramatically in both *rnpA49* mutants (Figure 5C, lanes 11–12). These results were consistent with the fact that three-fourth of the $tRNA^{Leu1}$ species were dependent on RNase P for maturation.

Since the half-life of the *valV valW* transcript increased dramatically following inactivation of RNase P (Figure 4), we performed a similar experiment to determine the half-life of the *leuQ leuP leuV* transcript. In this experiment, we used probe a (Figure 5A), since it hybridized to all the processing intermediates that were also detected by probes c and d (Figure 5A and C). As expected, no *leuQ leuP leuV* transcript was detected in both the wild type and *rne-1* mutant (Figure 6A). In contrast, all the processing intermediates that were observed under steady-state conditions (Figure 5C) were stabilized in both the *rnpA49* and *rne-1 rnpA49* mutants (Figure 6A and C). Interestingly, the QPV processing intermediate had a half-life of longer than 32 min in both strains (Figure 6A and C). In contrast, the levels of QP and pQ intermediates actually increased as a function of time in the *rnpA49* single mutant (Figure 6A and C). In the *rne-1 rnpA49* double mutant, the level of the QP intermediate was unaltered while pQ appeared to decay very slowly (Figure 6C). Furthermore, new decay intermediates (*) that were even smaller than the mature tRNA species accumulated over time in the *rnpA49* single mutant (Figure 6A), but were absent in the *rne-1 rnpA49* double mutant.

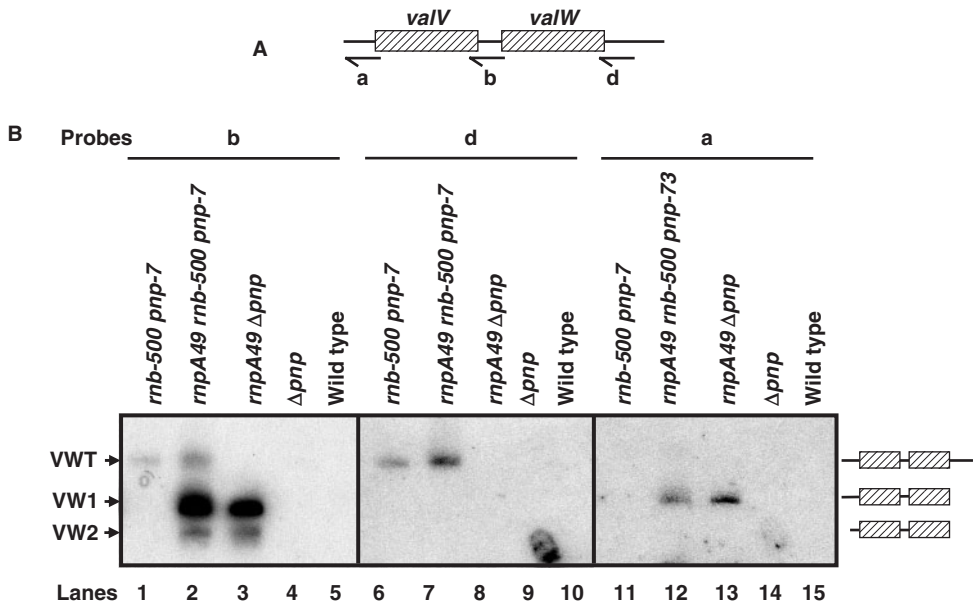

Figure 7. Northern analysis of the *valV valW* operon in exonuclease deficient strains. (**A**) Schematic represention of *valV valW* operon as described in Figure 2. (**B**) Autoradiograms of northern analysis. Total RNA (12 μg/lane) was separated on a 6% PAGE/8 M Urea gel, transferred to a nylon membrane and probed as described in the Materials and Methods section. The figure was composed from the same blot that was hybridized sequentially with probes b, d and a (A). The labeling efficiency of probe a was significantly lower than probe b (data not shown), resulting in detection of less VW1 by probe a. The genotypes of the strains used are listed above each lane. The names of each *valV valW* transcript (as explained in Figure 2B and the text) are indicated to the left and the corresponding graphical structures are indicated to the right.

PNPase and RNase II are involved in the removal of the terminator regions from the *valV valW* and *leuQ leuP leuV* precursor transcripts

Many tRNA transcripts are terminated in a Rho-independent fashion, which leads to the formation of a stem-loop structure with a very short single-stranded region at the 3′ terminus (6,8). Since the two major 3′ → 5′ exonucleases in *E. coli* (PNPase and RNase II) are both inhibited by secondary structures (35), this type of terminator sequence is generally thought to be removed endonucleolytically (6,8). However, both the *valV valW* and *leuQ leuP leuV* operons appear to be terminated in a Rho-dependent fashion since the downstream sequences do not contain any recognizable Rho-independent transcription terminator structures (data not shown). We hypothesized that this region would be susceptible to exonucleolytic degradation, explaining why we did not observe any hybridization with a probe specific for the sequences immediately downstream of the *valW* and *leuV* encoded CCA determinants in the experiments described above (probe d, Figure 2A; probe e, Figure 5A and data not shown).

Accordingly, we analyzed a northern blot of steady-state RNA isolated from strains that were deficient in PNPase, RNase II or a combination of PNPase, RNase II and RNase P using probes a, b and d for the *valV valW* operon (Figure 7A). As shown in Figure 7B, inactivation of PNPase (lanes 4 and 9), both PNPase and RNase P (lanes 3 and 8) or RNase II alone (CMA201/Δ*rnb*, data not shown) was not sufficient to detect the downstream sequences. In contrast, the loss of both PNPase and RNase II resulted in the detection of a precursor (VWT) (Figure 7B, lanes 1 and 6) that was approximately 35 nt larger than the VW1 species (Figure 7B, lanes 2 and 3). Inactivation of RNase P along with PNPase and RNase II increased the level (2.5 ± 0.1) of VWT (Figure 7B, lanes 2 and 7). Surprisingly, probe a (Figure 7A) did not hybridize to the VWT transcript (Figure 7B, lanes 11–12) suggesting that it was processed at the 5′ end by RNase E in a fashion similar to what occurred to generate the VW2 transcript (Figures 2B and 3). In addition, the ratio of VW1 to VW2 was significantly increased in strains that were deficient in both RNase P and one or more exonucleases (Figure 7B, lanes 2–3) compared to what was observed in the RNase P single mutant (Figure 2B, lanes 3 and 7).

Since the *leuQ leuP leuV* transcript has also been presumed to be terminated through a Rho-dependent mechanism (36), we tested to determine if its downstream sequences were also removed by a combination of RNase II and PNPase. In fact, a high molecular weight species that was ~40 nt longer than the QPV transcript (Figure 5C) was observed in strains that were deficient in either both exonucleases (PNPase and RNase II, SK5726) or both exonucleases and RNase P (SK10451) (data not shown).

DISCUSSION

The data presented here demonstrate for the first time the existence of a tRNA maturation pathway in *E. coli* that does not require RNase E. Specifically, for tRNA transcripts such as *valV valW* and *leuQ leuP leuV* only

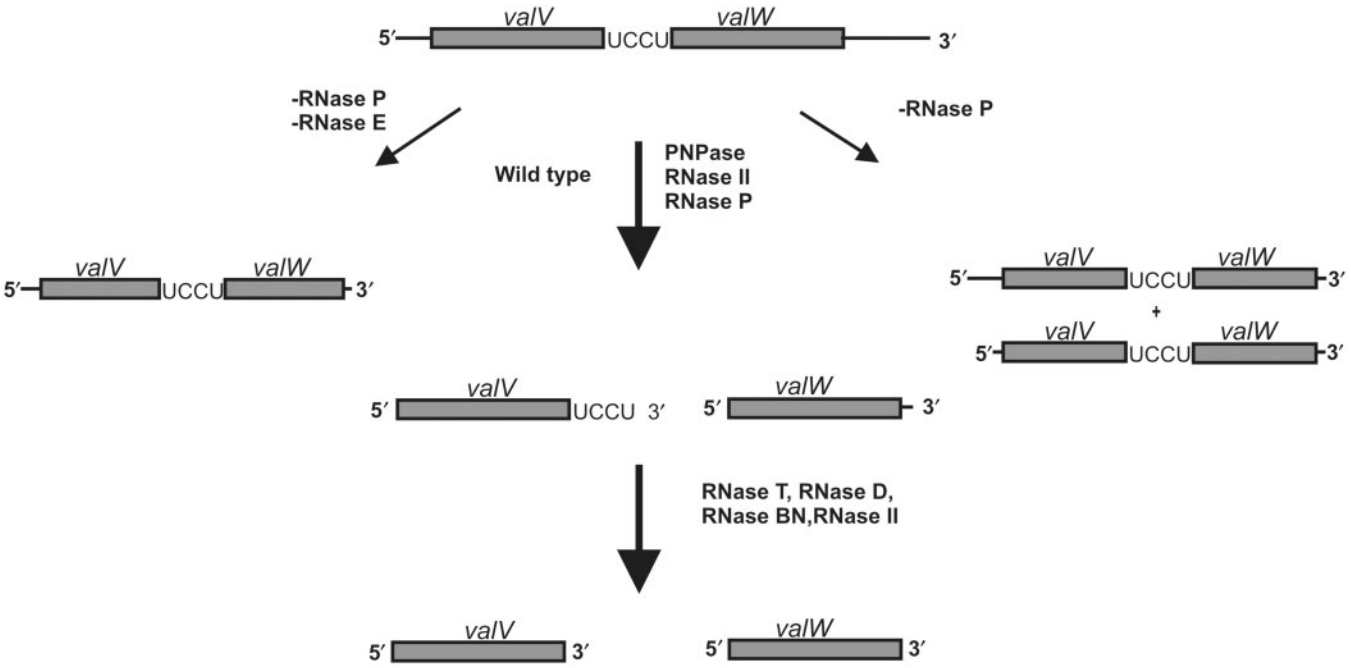

Figure 8. Model for RNase P-dependent maturation of *E. coli* tRNA precursors. RNase P-dependent pathway. In wild-type cells, RNase P cleaves at the 5′ mature termini of both *valV* and *valW*. The removal of the Rho-dependent transcription terminator sequences is dependent on PNPase, RNase II and possibly other ribonucleases (Figure 7). The extra nucleotides at the 3′ ends of both pre-tRNAs are removed by a combination of RNase T, RNase D, RNase PH, RNase BN and RNase II as suggested by the experiments of Li and Deutscher (3). Alternatively, it is possible that the action of PNPase and RNase II in removal of the Rho-dependent terminator sequences is sufficient to generate the mature 3′ terminus for *valW*. In the absence of RNase P, the 5′ end is cleaved inefficiently by RNase E (Figure 2B, 3, and 4), leading to the accumulation of a *valV valW* transcript with an unprocessed 5′ terminus (VW1, Figure 2B) and a slightly shorter transcript (VW2, Figure 2B) generated by the RNase E cleavage. In the absence of both RNase P and RNase E only the VW1 transcript is observed (Figure 2B). In the absence of RNase E alone, processing of this transcript occurs normally (Figure 2B and 4).

the endonucleolytic activity of RNase P is necessary to generate pre-tRNAs whose 5′ termini are already mature (Figure 8). The 3′ ends are subsequently processed exonucleolytically to produce functional tRNAs (Figure 8). Strong experimental support for this RNase E-independent maturation pathway is derived from the dramatic stabilization of polycistronic transcripts containing all the tRNAs in the absence of RNase P, but which are matured normally in the absence of RNase E (Figures 2 and 5). Furthermore, while the half-lives of the *valV valW* and *leuQ leuP leuV* transcripts were greater than 32 min in an *rnpA49* single mutant, they were estimated to be less than 30 s (see Materials and Methods section) in both wild-type and *rne-1* strains (Figures 4 and 6), showing that this pathway is very efficient.

Interestingly, it appears that the Rho-dependent transcription terminators associated with these operon transcripts are rapidly removed by a combination of PNPase and RNase II activity (Figure 7, data not shown), since the polycistronic transcripts that accumulated in the *rnpA49* and *rnpA49 rne-1* mutants no longer contained these sequences (Figures 2 and 5). However, even in a *rnpA49 pnp-7 rnb-500* strain (SK10451) most of the *valV valW* transcripts no longer contained the terminator sequences (Figure 7, lane 2). This observation may not be surprising since *E. coli* contains at least eight exoribonucleases that have considerable overlap in their functions (37).

However, all of our strains were defective in RNase PH (*rph-1*) and the levels of the transcript containing the terminator (VWT, Figure 7) in *pnp rnb* and *pnp rnb rnr* (RNase R) strains were identical (data not shown). Furthermore, it does not seem likely that RNase T, RNase D and RNase BN, all of which have limited substrate specificity, could account for this processing. In addition, the endonucleolytic removal of the terminator sequences by RNase E, in a fashion similar to what has been observed with Rho-independent transcription terminators (6,8), was ruled out by the fact that an *rne-1 rnpA49 pnp-7 rnb-500* strain had identical levels of the VWT transcript as observed in Figure 7, lane 2 (data not shown). Thus, we believe that there may be sufficient residual RNase II and/or PNPase activity in the *pnp-7 rnb-500* strains at the non-permissive temperature to account for the data in Figure 7. In fact, we have previously shown that there is a significant level of residual PNPase activity in a *pnp-7* strain (28).

Although $3' \rightarrow 5'$ exonucleolytic processing of the Rho-dependent terminator associated with the *trp* operon transcript has been predicted (38), this is the first direct demonstration of the involvement of both PNPase and RNase II in the removal of Rho-dependent transcription terminator sequences from the transcripts of tRNA operons, unlike the prediction of the Li and Deutscher model (6) (Figure 1), which invokes a cleavage by RNase

E to remove these sequences. This, in fact, may be the mechanism by which the downstream sequences of all 13 tRNA transcripts terminated in a Rho-dependent fashion are removed. Clearly, the involvement of PNPase and RNase II provides a distinctly different approach for terminator removal than what has been observed for tRNA transcripts terminated in a Rho-independent fashion [(6,8,11), Mohanty,B.K. and Kushner,S.R., unpublished data].

Since the data described above has demonstrated that there is more than one tRNA processing pathway in *E. coli*, the generally accepted model for tRNA processing (6,9,21) (Figure 1) most likely only correctly describes the maturation of a subset of tRNA operons such as *argX* [Figure 5B, (6,8)]. In fact, the RNase E cleavages that were observed here (Figures 2 and 5) only arose in the absence of RNase P, were not very efficient (Figures 4A and 6A), and occurred primarily in non-A/U-rich regions (Figure 3B). In addition, in the case of the *valV valW* transcript, the RNase E cleavages in the 5′ leader region were clearly a side reaction that resulted in a non-functional species. Similarly, for the *leuQ leuP leuV* transcripts some of the RNase E cleavages observed in the absence of RNase P generated products that were smaller than the mature $tRNA^{Leu}$ (Figure 6A, *), suggesting that they may serve as a form of quality control to prevent the build up of the unprocessed transcripts.

Surprisingly, the ability of RNase E to cleave the *valV valW* transcript appeared to be dependent on the presence of PNPase. For example, the amount of the VW2 species, which was generated by RNase E cleavages (Figures 2 and 3), was significantly reduced in strains lacking PNPase (Figure 7, lanes 2–3). This result suggests that the inefficient processing of the VW1 transcript in the absence of RNase P to generate VW2 requires the physical association of RNase E and PNPase, most probably through the multiprotein complex called the degradosome (39–41).

The highly efficient endonucleolytic separation and maturation of the tRNA transcripts from operons such as *valV valW* and *leuQ leuP leuV* by RNase P raises many important questions. It is currently believed that the pre-tRNA substrates generated by endonucleolytic cleavages of tRNA precursors become the substrates for the RNase P holoenzyme whereby the enzyme contacts the T-stem and loop of the pre-tRNA substrate, while the catalytic domain interacts with the acceptor stem and cleavage site (42,43). In fact, the non-tRNA substrates for RNase P [tmRNA, precursors to 4.5S RNA, viral mRNAs, C4 antisense RNA from bacteriophages P1 and P7 and transient structures within riboswitches (18,44–48)] very often closely resemble pre-tRNAs.

However, in the absence of initial RNase E cleavages within the *valV valW* and *leuQ leuP leuV* transcripts, it is not clear how RNase P recognizes these larger substrates. In fact, based on the secondary structures of the full-length transcripts that are predicted using the RNA-STAR program (49) (data not shown), it would appear that the RNase P cleavage sites at the mature 5′ ends of the individual tRNAs within the *valV valW* and *leuQ leuP leuV* transcripts may not correspond to known RNase P sites. Specifically, in the predicted equilibrium structures of both full-length transcripts, the RNase P cleavage sites fall within stem structures that should not be accessible to RNase P. Thus it is possible that the RNase P holoenzyme has greater flexibility in substrate recognition than previously envisioned. Alternatively, the maturation of multimeric tRNA substrates by RNase P may actually be coupled with transcription such that most of the precursors are cleaved prior to transcription termination. Interestingly, recent studies have suggested a role for the nuclear form of RNase P in transcription processing and regulation of tRNA gene expression in eukaryotes (50,51).

Furthermore, the notion that RNase P cannot act on tRNA substrates with long 3′ trailer sequences (23) needs to be reconsidered. In particular, if both operons are completely transcribed prior to any nucleolytic processing, the tRNA precursors will contain long 3′ trailer sequences. For example, the *leuQ leuP leuV* operon has intergenic regions of 29–34 nt with an observed size of over 300 nt (Figure 5). Yet, the data presented in Figure 5 shows that the half-life of this transcript is less than 30 s in the wild-type strain, indicating that it is an excellent substrate for RNase P.

It should be noted that the data presented in Figure 7 can also be interpreted to mean that most of the *valV valW* transcript is actually processed before transcription has been completed and that the full-length transcript only represents a small fraction of the total amount of *valV* and *valW* precursors that are transcribed. In this scenario, the failure to remove the terminator sequences generates a substrate that is resistant to RNase P cleavage such that the full-length transcript can be observed under steady-state conditions (Figure 7, lanes 1 and 6).

Finally, it is also worth revisiting the basis for why RNase P is essential for cell viability based on the results described above. It is currently thought that the enzyme is required to generate the mature 5′ ends for all tRNAs from any pre-tRNAs that contain extra nucleotides at their 5′ termini, since these may interfere with aminoacylation. However, *in vitro* studies indicate that the 5′ extension of yeast $tRNA^{Asp}$ does not interfere with recognition by aspartyl-tRNA synthetase (52). Furthermore, our recent observation that an *E. coli* mutant $tRNA^{Leu2}$ carrying an extra nucleotide (G) upstream of the mature 5′ end supports cell viability in a strain carrying a deletion of the chromosomally encoded *leuU* gene (53) suggests that aminoacylation of pre-tRNAs with immature 5′ ends may not be inhibitory (Mohanty,B.K., Bar-Peled,L. and Kushner,S.R., unpublished data). Accordingly, in the absence of RNase P, RNase E processed pre-tRNAs containing extra nucleotides at their 5′ termini but with mature 3′ termini may still be chargeable. In contrast, for those tRNAs that are completely dependent on RNase P for their maturation (e.g. *valV valW* and *leuQ leuP leuV* and probably others), there is no alternative processing pathway to generate a functional tRNA. Thus the loss of cell viability may arise not only from a general defect in the maturation of all tRNAs, but also more likely from the loss of a subset of tRNAs that are dependent on RNase P for endonucleolytic processing.

ACKNOWLEDGEMENTS

The authors wish to thank Liron Bar-Peled and Jamie Robinson for their assistance with strain constructions. This work was supported in part by a grant from the National Institute of General Medical Sciences (GM57220) to S.R.K. Funding to pay the Open Access publication charges for this article was provided by GM57220.

Conflict of interest statement. None declared.

REFERENCES

1. Blattner,F.R., Plunkett,G.III, Bloch,C.A., Perna,N.T., Burland,V., Riley,M., Collado-Vides,J., Glasner,J.D., Rode,C.K. *et al.* (1997) The complete sequence of *Escherichia coli* K-12. *Science*, **277**, 1453–1474.
2. Li,Z., Pandit,S. and Deutscher,M.P. (1998) 3′ Exoribonucleolytic trimming is a common feature of the maturation of small, stable RNAs in *Escherichia coli*. *Proc. Natl Acad. Sci. USA*, **95**, 2856–2861.
3. Li,Z. and Deutscher,M.P. (1994) The role of individual exoribonucleases in processing at the 3′ end of *Escherichia coli* tRNA precursors. *J. Biol. Chem.*, **269**, 6064–6071.
4. Li,Z. and Deutscher,M.P. (1996) Maturation pathways for *E. coli* tRNA precursors: a random multienzyme process *in vivo*. *Cell*, **86**, 503–512.
5. Altman,S., Kirsebom,L. and Talbot,S. (1995) Recent studies of RNase P. In Soll,D. and RajBhandary, (eds), *tRNA: Structure and Function*, American Society for Microbiology Press, Washington, DC, pp. 67–78.
6. Li,Z. and Deutscher,M.P. (2002) RNase E plays an essential role in the maturation of *Escherichia coli* tRNA precursors. *RNA*, **8**, 97–109.
7. Soderbom,F., Svard,S.G. and Kirsebom,L.A. (2005) RNase E cleavage in the 5′ leader of a tRNA precursor. *J. Mol. Biol.*, **352**, 22–27.
8. Ow,M.C. and Kushner,S.R. (2002) Initiation of tRNA maturation by RNase E is essential for cell viability in *Escherichia coli*. *Genes Dev.*, **16**, 1102–1115.
9. Deutscher,M.P. (2006) Degradation of RNA in bacteria: comparison of mRNA and stable RNA. *Nucleic Acids Res.*, **34**, 659–666.
10. Deana,A. and Belasco,J.G. (2003) The function of RNase G in *Escherichia coli* is constrained by its amino and carboxyl termini. *Mol. Microbiol.*, **51**, 1205–1217.
11. Mohanty,B.K. and Kushner,S.R. (2007) Rho-independent transcription terminators inhibit RNase P processing of the *secG leuU* and *metT* polycistronic transcripts in *Escherichia coli*. *Nucleic Acids Res.*, in press.
12. Stark,B.C., Kole,R., Bowman,E.J. and Altman,S. (1977) Ribonuclease P: an enzyme with an essential RNA component. *Proc. Natl Acad. Sci. USA*, **75**, 3719–3721.
13. Guerrier-Takada,C., Gardiner,K., Marsh,T., Pace,N. and Altman,S. (1983) The RNA moiety of ribonuclease P is the catalytic subunit of the enzyme. *Cell*, **35**, 849–857.
14. Gopalan,V., Vioque,A. and Altman,S. (2002) RNase P: variations and uses. *J. Biol. Chem.*, **277**, 6759–6762.
15. Kirsebom,L.A., Baer,M.F. and Altman,S. (1988) Differential effects of mutations in the protein and RNA moieties of RNase P on the efficiency of suppression by various tRNA suppressors. *J. Mol. Biol.*, **204**, 879–888.
16. Sakano,H., Yamada,S., Ikemura,T., Shimura,Y. and Ozeki,H. (1974) Temperature sensitive mutants of *Escherichia coli* for tRNA synthesis. *Nucleic Acids Res.*, **1**, 355–371.
17. Ikemura,T., Shimura,Y., Sakano,H. and Ozeki,H. (1975) Precursor molecules of *Escherichia coli* transfer RNAs accumulated in a temperature-sensitive mutant. *J. Mol. Biol.*, **96**, 69–86.
18. Alifano,P., Rivellini,F., Piscitelli,C., Arraiano,C.M., Bruni,C.B. and Carlomagno,M.S. (1994) Ribonuclease E provides substrates for ribonuclease P-dependent processing of a polycistronic mRNA. *Genes Dev.*, **8**, 3021–3031.
19. Li,Y., Cole,K. and Altman,S. (2003) The effect of a single, temperature-sensitive mutation on global gene expression in *Escherichia coli*. *RNA*, **9**, 518–532.
20. Ilgen,C., Kerik,L.L. and Carbon,J. (1976) Isolation and characterization of large transfer ribonucleic acid precursors from *Escherichia coli*. *J. Biol. Chem.*, **251**, 922–929.
21. Li,Z., Gong,X., Joshi,V.H. and Li,M. (2005) Co-evolution of tRNA 3′ trailer sequences with 3′ processing enzymes in bacteria. *RNA*, **11**, 567–577.
22. Schedl,P. and Primakoff,P. (1973) Mutants of *Escherichia coli* thermosensitive for the synthesis of transfer RNA. *Proc. Natl Acad. Sci. USA*, **70**, 2091–2095.
23. Altman,S., Baer,M.F., Gold,H., Guerrier-Takada,C., Lawrence,N., Lumelsky,N. and Vioque,A. (1987) Cleavage of RNA by RNase P. In Inouye,M. and Dudock,B. S. (eds), *Molecular Biology of RNA*, Academic Press, Orlando, pp. 3–15.
24. Kelly,K.O., Reuven,N.B., Li,Z. and Deutscher,M.P. (1992) RNase PH is essential for tRNA processing and viability in RNase-deficient *Escherichia coli* cells. *J. Biol. Chem.*, **267**, 16015–16018.
25. Deutscher,M.P. and Li,Z. (2001) Exoribonucleases and their multiple roles in RNA metabolism. *Prog. Nucleic Acids Res.*, **66**, 67–105.
26. Arraiano,C.M., Yancey,S.D. and Kushner,S.R. (1988) Stabilization of discrete mRNA breakdown products in *ams pnp rnb* multiple mutants of *Escherichia coli* K-12. *J. Bacteriol.*, **170**, 4625–4633.
27. Ono,M. and Kuwano,M. (1979) A conditional lethal mutation in an *Escherichia coli* strain with a longer chemical lifetime of mRNA. *J. Mol. Biol.*, **129**, 343–357.
28. Mohanty,B.K. and Kushner,S.R. (2003) Genomic analysis in *Escherichia coli* demonstrates differential roles for polynucleotide phosphorylase and RNase II in mRNA abundance and decay. *Mol. Microbiol.*, **50**, 645–658.
29. Cairrao,F., Chora,A., Zilhao,R., Carpousis,A.J. and Arraiano,C.M. (2001) RNase II levels change according to the growth conditions: characterization of *gmr*, a new *Escherichia coli* gene involved in the modulation of RNase II. *Mol. Microbiol.*, **39**, 1550–1561.
30. Piedade,J., Zilhao,R. and Arraiano,C.M. (1995) Construction and characterization of an absolute deletion of *Escherichia coli* ribonuclease II. *FEMS Microbiol. Lett.*, **127**, 187–193.
31. Donovan,W.P. and Kushner,S.R. (1986) Polynucleotide phosphorylase and ribonuclease II are required for cell viability and mRNA turnover in *Escherichia coli* K-12. *Proc. Natl Acad. Sci. USA*, **83**, 120–124.
32. O'Hara,E.B., Chekanova,J.A., Ingle,C.A., Kushner,Z.R., Peters,E. and Kushner,S.R. (1995) Polyadenylylation helps regulate mRNA decay in *Escherichia coli*. *Proc. Natl Acad. Sci. USA*, **92**, 1807–1811.
33. Sambrook,J., Fritsch,E.F. and Maniatis,T. (1989) *Molecular cloning, a laboratory manual 2nd edn*. Cold Spring Harbor Laboratory Press, Cold Spring Harbor, NY.
34. Mohanty,B.K. and Kushner,S.R. (1999) Residual polyadenylation in poly(A) polymerase I (*pcnB*) mutants of *Escherichia coli* does not result from the activity encoded by the *f310* gene. *Mol. Microbiol.*, **34**, 1109–1119.
35. Spickler,C. and Mackie,G.A. (2000) Action of RNase II and polynucleotide phosphorylase against RNAs containing stem-loops of defined structure. *J. Bacteriol.*, **182**, 2422–2427.
36. Duester,G., Campen,R.K. and Holmes,W.M. (1981) Nucleotide sequence of an *Escherichia coli* tRNA (Leu 1) operon and identification of the transcription promotion signal. *Nucleic Acids Res.*, **9**, 2121–2139.
37. Deutscher,M.P. (1993) Promiscuous exoribonucleases of *Escherichia coli*. *J. Bacteriol.*, **175**, 4577–4583.
38. Mott,J.E., Galloway,J.L. and Platt,T. (1985) Maturation of *Escherichia coli* tryptophan operon mRNA: evidence for 3′ exonucleolytic processing after rho-dependent termination. *EMBO J.*, **4**, 1887–1891.
39. Carpousis,A.J., Van Houwe,G., Ehretsmann,C. and Krisch,H.M. (1994) Copurification of *E. coli* RNAase E and PNPase: evidence for a specific association between two enzymes important in RNA processing and degradation. *Cell*, **76**, 889–900.
40. Py,B., Causton,H., Mudd,E.A. and Higgins,C.F. (1994) A protein complex mediating mRNA degradation in *Escherichia coli*. *Mol. Microbiol.*, **14**, 717–729.
41. Py,B., Higgins,C.F., Krisch,H.M. and Carpousis,A.J. (1996) A DEAD-box RNA helicase in the *Escherichia coli* RNA degradosome. *Nature*, **381**, 169–172.

42. Walker,S.C. and Engelke,D.R. (2006) Ribonuclease P: the evolution of an ancient RNA enzyme. *Crit. Rev. Biochem. Mol. Biol.*, **41**, 77–102.
43. Christian,E.L., Zahler,N.H., Kaye,N.M. and Harris,M.E. (2002) Analysis of substrate recognition by the ribonucleoprotein RNase P. *Methods*, **28**, 307–322.
44. Mans,R.M.W., Guerrier-Takada,C., Altman,S. and Pleij,C.W.A. (1990) Interaction of RNase P from *Escherichia coli* with pseudoknotted structures in viral RNAs. *Nucleic Acids Res.*, **18**, 3479–3487.
45. Hartmann,R.K., Heinrich,J., Schlegl,J. and Schuster,H. (1995) Precursor of C4 antisense RNA of bacteriophages P1 and P7 is a substrate for RNase P of *Escherichia coli*. *Proc. Natl Acad. Sci. USA*, **92**, 5822–5826.
46. Peck-Miller,K.A. and Altman,S. (1991) Kinetics of the processing of the precursor to 4.5S RNA, a naturally occurring substrate for RNase P from *Escherichia coli*. *J. Mol. Biol.*, **221**, 1–5.
47. Altman,S., Wesolowski,D., Guerrier-Takada,C. and Li,Y. (2005) RNase P cleaves transient structures in some riboswitches. *Proc. Natl Acad. Sci. USA*, **102**, 11284–11289.
48. Komine,Y., Kitabatake,M., Yokigawa,T., Nishikawa,K. and Inokuchi,H. (1994) A tRNA-like structure is present in 10Sa RNA, a small stable RNA from *Escherichia coli*. *Proc. Natl Acad. Sci. USA*, **91**, 9223–9227.
49. Gultyaev,A.P., van Batenburg,F.H.D. and Pleij,C.W.A. (1995) The computer simulation of RNA folding pathways using a genetic algorithm. *J. Mol. Biol.*, **250**, 37–51.
50. Jarrous,N. and Reiner,R. (2007) Human RNase P: a tRNA-processing enzyme and transcription factor. *Nucleic Acids Res.*, **35**, 3519–3524.
51. Reiner,R., Ben-Asouli,Y., Krilovetzky,I. and Jarrous,N. (2006) A role for the catalytic ribonucleoprotein RNase P in RNA polymerase III transcription. *Genes Dev.*, **20**, 1621–1635.
52. Perret,V., Florentz,C. and Giege,R. (1990) Efficient aminoacylation of a yeast transfer RNA^{Asp} transcript with a 5′ extension. *FEBS Lett.*, **270**, 4–8.
53. Nishiyama,K. and Tokuda,H. (2005) Genes coding for SecG and Leu2-tRNA form an operon to give an unusual RNA comprising mRNA and a tRNA precursor. *Biochim. Biophys. Acta*, **1729**, 166–173.